Scaling properties of heavy rainfall at short duration: A regional analysis

D. Ceresetti, G. Molinié, J.-D. Creutin

Scaling properties of heavy rainfall at short duration: A regional analysis

D. Ceresetti,[1] G. Molinié,[1] and J.-D. Creutin[1]

Received 2 September 2009; revised 29 January 2010; accepted 4 June 2010; published 25 September 2010.

[1] The aim of this paper is to assess the scaling properties of heavy point rainfall with respect to duration. In the region of interest, the probability distribution tails of hourly to daily rainfall display log-log linearity. The log-log linearity of tails is a feature of fat-tailed distributions. The conservation of this property throughout the scales will be investigated in the framework of scale-invariant analysis. Evidence of the scaling of heavy rainfall is shown for one particularly long rainfall series through the conservation of the survival probability shape at durations in the range 1–24 h. An objective method is implemented to estimate the hyperbolic-tail parameters of rainfall distributions. This method is automatized and detects the lower bound above which the distributions exhibit power law tails and determines the power law exponent α using a maximum likelihood estimator. The application of unbiased estimation methods and scale-invariant properties for the estimation of the power law exponent provides a significant reduction of the intergage power law variability. This achievement is essential for a correct use of geostatistical approaches to interpolate the power law parameters at ungaged sites. The method is then applied to the rain gage network in the Cévennes-Vivarais region, a Mediterranean mountainous region located in southern France. The maps show thicker rainfall distribution tails in the flat area between the seashore and the foothill. It is shown that in a flat region closer to the Mediterranean Sea the rainfall distribution tails are hyperbolic and the power law exponent is quasi-constant with duration, whereas, over the mountain, the power law behavior is less defined. The physical reasons for such results and the consequences for the statistical modeling of heavy rainfall are then discussed, providing an innovative point of view for the comprehension of the rainfall extremes behavior at different temporal scales.

Citation: Ceresetti, D., G. Molinié, and J.-D. Creutin (2010), Scaling properties of heavy rainfall at short duration: A regional analysis, *Water Resour. Res.*, *46*, W09531, doi:10.1029/2009WR008603.

1. Introduction

[2] During the last thirty years, a considerable body of investigations analyzed the scale invariance of rainfall, demonstrating that rainfall fields have intrinsic scaling properties within a specified range of scales. A physical process is scale invariant if its probability distribution, once applied a rescaling factor, does not change under scale magnification or contraction within a given range.

[3] *Frisch and Parisi* [1985] provided fundamental insights into the multiscaling behavior of processes. Analyzing the average value of the qth power of the change in the turbulent velocity for different time lags, they found that $|v(h) - v(h + l)|^q$ varies as the power law $l^{\zeta(q)}$, where ζ is nonlinear with q. The nonlinearity of $\zeta(q)$ indicates that the velocity fluctuations display multifractal scaling. A Legendre transform allows to switch from the moment scaling function to the codimension function $c(\gamma)$, describing the scaling in terms of probability distribution. The singularity order γ in the codimension function expression is the dual of the moment order q in the moment scaling function.

[4] A particular case of scaling, referred to as simple scaling, occurs when the scaling exponent $\zeta(q)$ is linear with q. In simple scaling processes the probability distribution is rescaled from a scale to another by means of a single scaling exponent, while in multifractality the scaling exponent depends on the degree of singularity of the process. The distribution equality between two probability distributions at different scales is referred to as "strict sense scaling." A weaker property is usually adopted for assessing the scaling behavior of a process: the equality of moments, referred to as "wide sense scaling" [*Gupta and Waymire*, 1990].

[5] First evidences of the multiscaling behavior of meteorological fields were shown by *Schertzer and Lovejoy* [1987] analyzing meteorological radar reflectivities. *Gupta and Waymire* [1990] evaluated and detailed the different types of scaling of instantaneous radar rainfall with respect to the surface. The multiscaling concept can be also applied to time series of rain gage data over a wide range of temporal scales. *Ladoy et al.* [1993] analyzed a pluviometric series located in Nîmes (France) covering 50 years of data characterized at a 12 h time resolution. They have been able

[1]Laboratoire d'Étude des Transfert en Hydrologie et Environnement, Université de Grenoble, CNRS, INPG, IRD, UJF, Grenoble, France.

0043-1397/10/2009WR008603

to determine the multifractal parameters of the rainfall series finding scale invariance in the range 12 h to 16 days. *Hubert et al.* [1993] analyzed data from different regions at temporal scales of 6 min at the Reunion Island (Indian Ocean), of 15 min in the French Alps, of 1 day at Nîmes and at Dédougou (Burkina Faso, West Africa). They found out multiple scaling behavior of point rainfall rates from one to several days (16–30 days depending on the location).

[6] The scale invariance of rainfall maxima has been the topic of several studies. *Bendjoudi et al.* [1997] derived a multifractal based intensity-duration-frequency formulation showing that a multifractal phase transition implies algebraic tails above a given singularity level. From the direct analysis of rainfall data series, *Burlando and Rosso* [1996], *Menabde et al.* [1999], and *Borga et al.* [2005] showed that the annual maxima are approximately simple scaling in the range 0.5–24 h. It is worth mentioning that *Burlando and Rosso* [1996] and *Menabde et al.* [1999] processed data series from different climatic regions. In work by *Burlando and Rosso* [1996], one rain gage station is located in a flat area whereas the second is a mountainous station. *Menabde et al.* [1999] dealt with a midlatitude temperate region of Australia and with a semiarid region of South Africa.

[7] The usual approach for the analysis of heavy rainfall is based on the extreme value theory. This theory considers events exceeding a given threshold (peak over threshold (POT)) or maxima during a given period (annual or shorter periods; see *Kotz and Nadarajah* [2000] for more details), resulting in two distribution classes: generalized Pareto distributions (GPD) and generalized extreme value (GEV) distributions. The GEV distribution class involves three types of maxima: hyperbolic-tailed (GEV-II), exponential (GEV-I) and bounded maxima (GEV-III). Maxima rainfall rates usually follow GEV-I (Gumbel) or GEV-II (Fréchet) distributions [*Kottegoda and Rosso*, 1997], depending on the decay of the probability distribution (respectively exponential and hyperbolic tailed, hyperbolic tails being thicker than exponential ones). Daily rainfall maxima are often modeled with Gumbel distributions [*Gumbel*, 1958; *Koutsoyiannis et al.*, 1998]. Nevertheless, infradaily rainfall can show thicker tails and the improper use of GEV-I distribution leads to a generalized underestimation of extreme events for high return periods. The choice between the two approaches (hyperbolic or exponential tailed distributions) has been justified only by empirical evidence on the distribution of maxima.

[8] Few studies on heavy rainfall scaling focused on the properties of the underlying probability distributions. *Hubert and Bendjoudi* [1996] studied the distribution of heavy rainfall in Dédougou over scales ranging from 1 day to 1 year. Analyzing the power law exponent α in double-logarithmic plot, they showed that the hyperbolic tail of the pdf does not change with the accumulation period, resulting in simple scaling of rainfall extremes. Approximate simple scaling is also illustrated in Table 3 of *Sivakumar* [2000] analyzing the hyperbolic tail of the probability distributions for accumulation durations between 6 h and 7 days for two rainfall series at Singapore and Leaf River Basin (Mississippi, USA).

[9] In this paper, our purpose is to give a regional description of heavy rainfall statistics. According to our knowledge, no study focused on the intergage properties of the probability distribution tails. Many papers focused on the behavior of single rain gages, not representative of a complex-relief region. Applying an objective method for determining the power law exponent α, and a scale-invariant relationship that involves the hyperbolic tail of the distribution, our aim is to reduce the intergage variability of the power law parameters. According to our experience, the determination of the power law parameters using an arbitrary threshold–based method prevents a robust parameter estimation and thus the comparison between gages and the regionalization of the variable. Applying the method to about two hundred stations, we show that a coherent interpolation process is now possible as well as the prediction of the tail behavior at ungaged sites.

[10] The paper is structured as follows: we first show evidence of hyperbolic behavior of heavy rainfall at specific stations and we describe the objective method implemented in order to determine the hyperbolic model parameters (section 2). In section 3, we use a reference rainfall series (50 years) to check for the simple scaling properties of distribution tails between 1 and 24 h. The goal of section 4 is to map the model parameters of heavy rainfall. A comparison of the power law exponent α at accumulation durations from 1 h to 8 h allows us to identify subregions where α is approximately constant. The results related to the rainfall-forcing processes and to the extreme value theory are discussed in section 5.

2. Heavy Point Rainfall Behavior

[11] In this section, we characterize the positive rainfall rates by their survival probability (complement to 1 of the cumulative distribution function). The decay of the survival probability gives information about the underlying law of extremes; the region of interest is shown in Figure 1. An example of the survival probability of hourly point rainfall is plotted in Figure 2 for the rain gage station of Colognac, about 30 km SW of Alés, France. As we are interested in heavy rainfall, the plot is limited to the upper 5% of the observations. The survival probability tail is hyperbolic. It can be parameterized by a decay rate α and by a lower bound $x_{\min}$. In practice, the decay rate is usually estimated by fitting a power law to the data (i.e., a straight line on a log-log plot) and calculating its slope. However, this particular fitting process is influenced by the empirical estimation of the survival probability. One can see that the empirical survival probability of the highest observations on the log-log plot in Figure 2 diverges from the straight line. As illustrated in the following simple exercise, this can be interpreted as a consequence of the mode of computation of the highest empirical frequencies (outliers). Taking $N = 100$ realizations of a random variable X, the empirical survival probability can be defined, if we take the Weibull plotting position expression, by

$$P(X > x) = 1 - \frac{i}{N+1}, \tag{1}$$

where i is the rank of a sorted sample x, varying from 1 to N. Let us consider to add one further observation to the series. If this observation is the highest of the sample, it will be ranked 101 in the sorted sample. The survival probability of the 100-ranked sample will be modified by 100%, passing from 0.01 to about 0.02. At the same time, the survival probability of the 50-ranked sample will be modified by only 0.5%, passing from about 0.5 to about 0.495. This

(a)

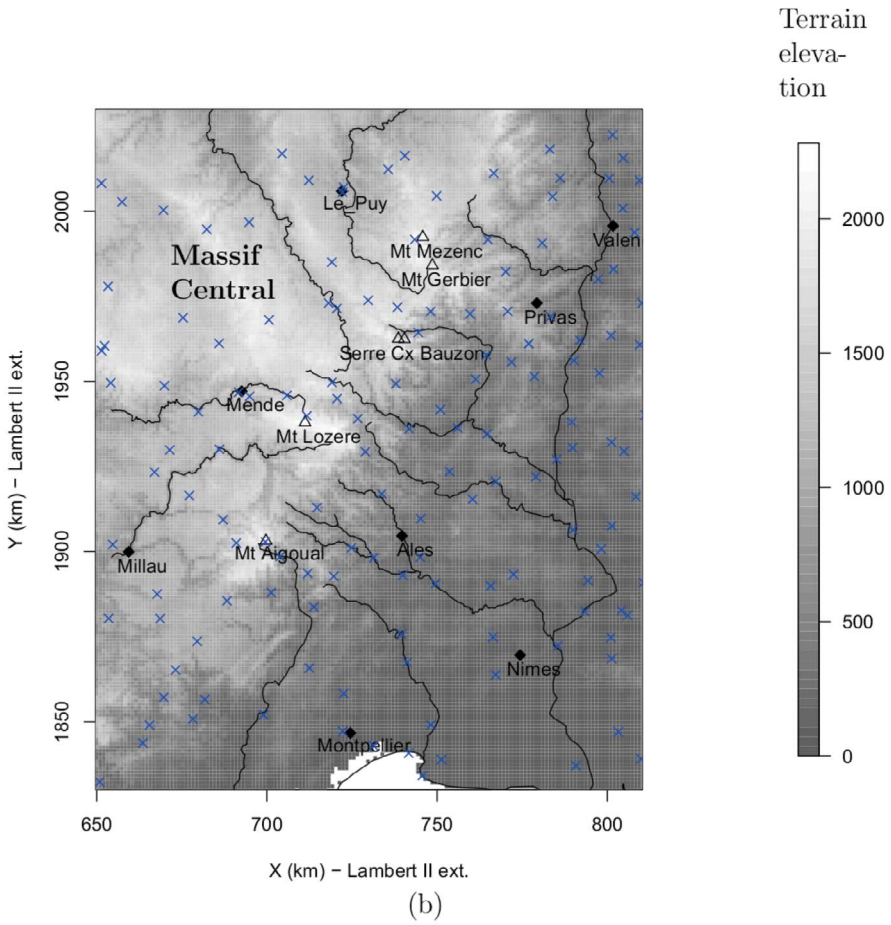

(b)

Figure 1. (a) Localization of the region of interest. (b) Elevation map (gray shaded area in m above sea level) in the region of interest. The crosses indicate the hourly rain gage network. The solid line indicates the main hydrographic network. The main river in the region is the Rhône River. It roughly represents the eastern boundary of the region. The Mediterranean shore is the southern boundary, and the mountain ridge, oriented north-northwest, is the southern limit of the Massif Central plateau.

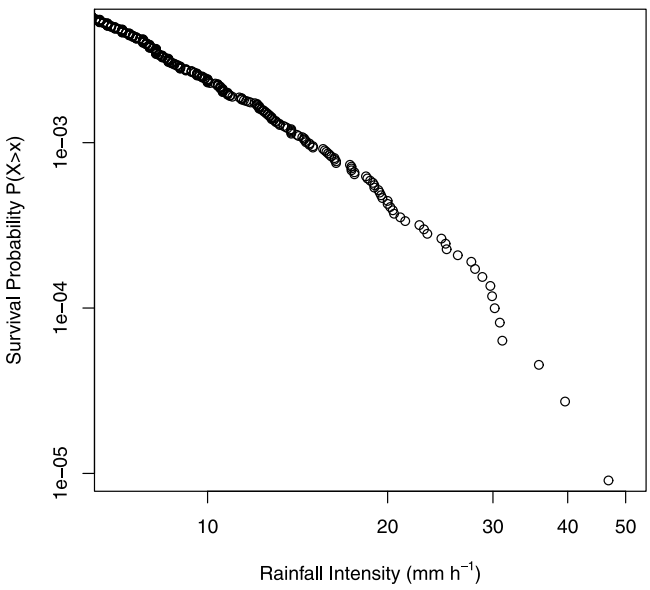

Figure 2. Log-log plot of the survival probability distribution of hourly rainfall for the rain gage station of Colognac, France.

exercise highlights that empirical survival probabilities are robustly estimated when looking at usual probability levels, but strongly biased when dealing with extreme quantiles. The bias of a plotting position formula depends on the probability distribution of the sample. More adapted expressions for the determination of the plotting position in positively skewed data are available for several probability distributions [*Kottegoda and Rosso*, 1997], and the exercise above can be easily generalized for any of these.

[12] This example highlights that any power law fitting method based on the plotting of empirical cumulative density function is affected by large uncertainties, which increase in presence of outliers in the probability distribution. *Goldstein et al.* [2004] showed the inaccuracy of some of these graphical methods by calculating the bias in the estimation of the power law exponent α of samples composed by 10000 realizations. They found out that the maximum likelihood estimator (MLE) provides a better estimate $\hat{\alpha}$ than other methods, including least squares linear regression (LSq). The MLE estimator (equation (2)) is equivalent to the Hill estimator adopted in extreme value theory:

$$\hat{\alpha} = 1 + n\left[\sum_{i=1}^{n} \ln \frac{x_i}{X_{\min}}\right]^{-1}. \tag{2}$$

[13] The main advantage using MLE with respect to LSq is that the method provides an unbiased estimate of the exponent $\hat{\alpha}$, independently of the empirical cumulative distribution. We performed complementary simulations to extend the numerical experiment of *Goldstein et al.* [2004] to shorter series (sets of about 1000 realizations) drawn from a Pareto distribution:

$$P(X \geq x) = \left(\frac{x}{x_{\min}}\right)^{-\alpha}, \tag{3}$$

for all $x \geq x_{\min}$, where $x_{\min}$ is the so-called scale parameter and α the shape parameter. One hundred series with $x_{\min}$ = 10 and α = 3 have been generated with N, the number of realizations, ranging from 100 to 10000. In Figure 3 the box plots summarize the distributions of the estimated $\hat{\alpha}$ computed using, respectively, the LSq and MLE methods. Considering a set of 10000 samples, we notice that LSq provides far more scattered estimations of $\hat{\alpha}$ than MLE, in

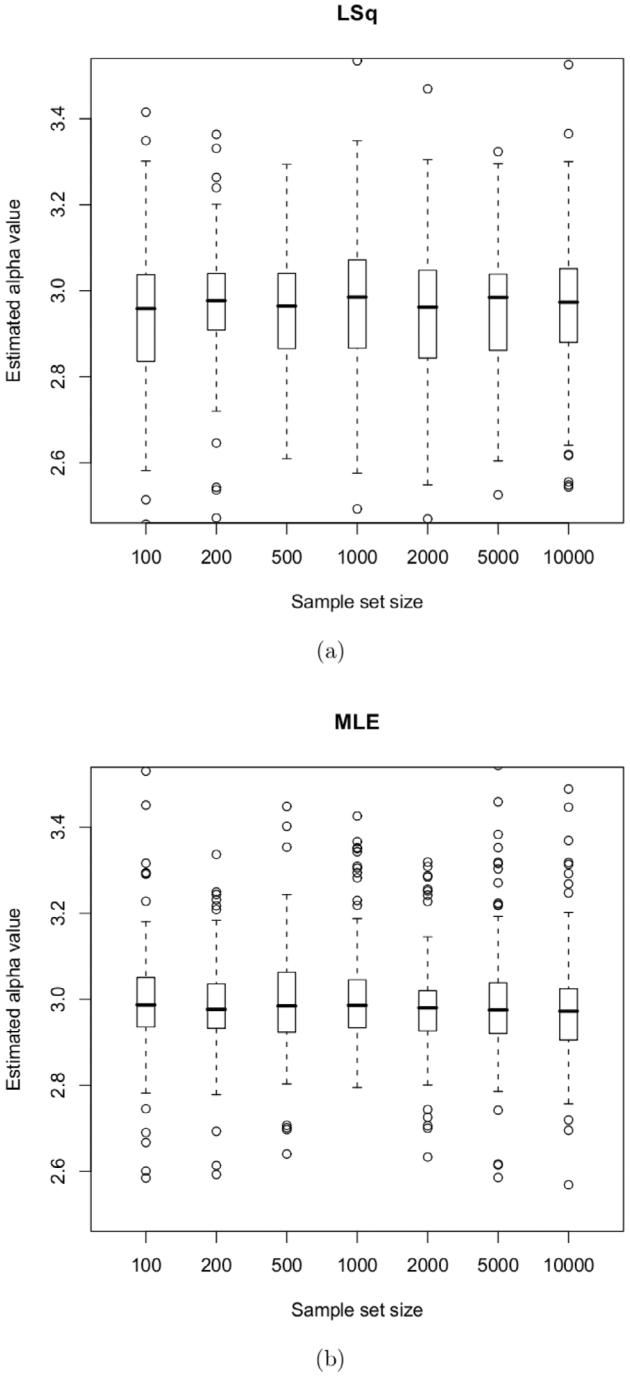

Figure 3. Box plots of the distribution of $\hat{\alpha}$ using (a) the least squares fitting and (b) the maximum likelihood estimator on 100 samples of different size. All the samples were distributed following a Pareto distribution, $x_{\min}$ = 10, k = 3.

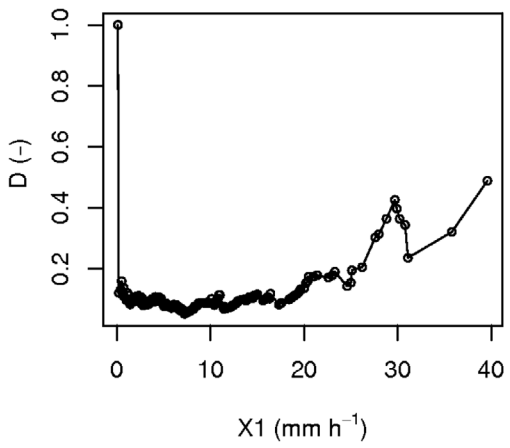

Figure 4. Plot of the Kolmogorov-Smirnov D statistics as a function of the lower bound x_1 for the hourly rain gage station of Colognac, France (see Figure 2). The minimum of D corresponds to $x_{\min}$, which is used in turn to determine α.

agreement with *Goldstein et al.* [2004]; the dispersion of $\hat{\alpha}$ remains of the same order of magnitude whatever the sample set size. Moreover, the average of $\hat{\alpha}$ estimated by MLE remains close to 3 (the actual value), while it is more fluctuating when estimated by LSq. This confirms that MLE is a more consistent estimator than LSq. Two reasons have been highlighted in literature. First, LSq is more sensitive to the presence of outliers in the distribution tails. Second, the residuals of the linear fitting of log-reduced variables do not follow a Gaussian distribution [*Clauset et al.*, 2009].

[14] After having defined an unbiased method for the estimation of the power law exponent of hyperbolic distributions, the second major problem is to define the scale parameter ($x_{\min}$ in equation (3)), i.e., the lower bound above which the power law holds. Considering an arbitrary bound, as we did in Figure 2, is obviously not satisfactory. The determination of $\hat{\alpha}$ depends on the choice of the lower bound $\hat{x}_{\min}$. This bound can be different from one rain gage to another, because of the heterogeneity of the rainfall regime in the region. *Clauset et al.* [2009] derived a method to estimate the lower bound $\hat{x}_{\min}$.

[15] The probability density function of a variable y assuming discrete values and distributed as a power law is defined as [*Goldstein et al.*, 2004]

$$p(x) = \frac{x^{-\alpha}}{\zeta(\alpha, x_{\min})}, \tag{4}$$

where α is the power law exponent and $\zeta(\alpha, x_{\min})$ is the generalized Zeta function, defined as

$$\zeta(\alpha, x_{\min}) = \sum_{n=0}^{\infty} (n\Delta x + x_{\min})^{-\alpha}, \tag{5}$$

where $x_{\min}$ is the lower bound and Δx is the rain gage accuracy (0.1 mm of rain depth for the analyzed rain gage database).

[16] The estimated lower bound $\hat{x}_{\min}$ is determined by means of the Kolmogorov-Smirnov (KS) statistics. *Clauset et al.* [2009] have shown that this objective method is among the most efficient for comparing two distributions. The D statistics of the KS test is defined as

$$D = \max_{x \geq x_1} |S(x) - P(x)|, \tag{6}$$

where $S(x)$ and $P(x)$ are the cumulative probability distributions of the observed samples and of the model, above a lower bound x_1. Figure 4 shows the D statistics as a function of x_1 for the rain gage of Colognac. The value of x_1 corresponding to the minimum of D provides the estimated $\hat{x}_{\min}$, 7.2 mm h^{-1} in the case shown in Figure 4. Therefore, $\hat{\alpha}$ is estimated applying MLE to the X realizations higher or equal to $\hat{x}_{\min}$.

[17] Figure 5 illustrates the sensitivity of $\hat{\alpha}$ to x_1. For x_1 higher than 20 mm h^{-1} the $\hat{\alpha}$ sensitivity to x_1, as well as the estimation uncertainty, is consistently high. This is the result of the rapid decrease of the sample set size, and in this method, as well as in other methods, α is never taken in this range. For values of x_1 close to the optimal value $\hat{x}_{\min}$, i.e. within the range 0.1–15 h^{-1}, the sensitivity of $\hat{\alpha}$ is considerably lower, varying of some decimals. However, it is worthy to notice that small variations of $\hat{\alpha}$ can have relevant influence in the estimation of rainfall for very high quantiles.

3. Scaling Behavior of Heavy Rainfall

[18] In section 2, we stated that the tail distribution of hourly rainfall behaves as a power law at many rain gage stations and we described a method to estimate the power law parameters. In the current section, we investigate the conservation of this property for temporal resolutions ranging from 1 to 24 h, for the longest hourly rain gage series of the region, located in Montpellier (see Figure 1). This rain gage collected over 50 years of hourly data, in the period 1920–1972. This rain gage has been used for testing some of the properties that we assume throughout the paper. Rainfall rates for four durations (1, 4, 10 and 24 h) have been computed by aggregation within nonoverlapping windows. To make possible their scale-free intercomparison, the sample sets are first normalized by the mean rainfall rate, subsequently, for each duration, a sample with fixed size is chosen (2000 nonzero samples).

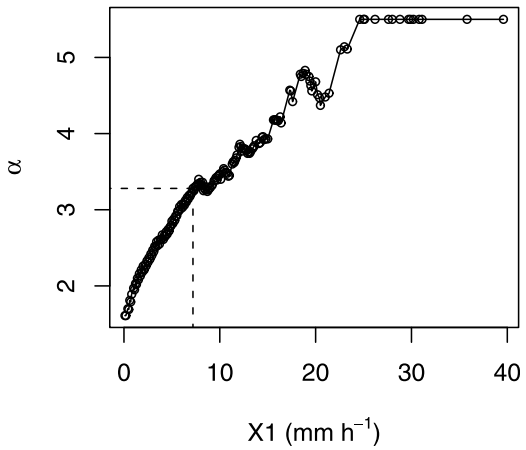

Figure 5. Power law exponent α as a function of the lower bound x_1 for the rain gage station of Colognac, France (see Figure 2).

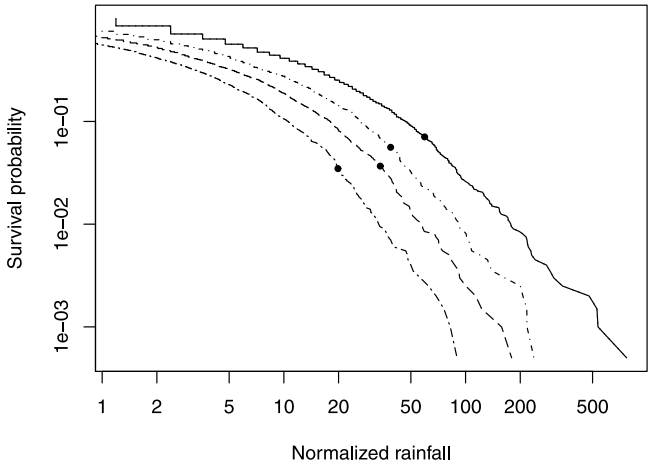

Figure 6. Log-log plot of survival probability of the normalized rainfall rate for durations of 1 h (solid line), 4 h (dash-dotted line), 10 h (dashed line) and 24 h (long-dash-dotted line) at the rain gage station of Montpellier-Bel Air. A solid circle marks the lower bounds $x_{\min}$.

[19] The assumption of data stationarity is often required to analyze the heavy rainfall behavior. On the other hand, the sample set size has to be as long as possible to improve the robustness of the statistics. These two requirements could be incompatible. The stationarity of the rainfall intensities of the 50 year long data set of Montpellier is thus questionable. Therefore, we have checked this stationarity in computing the survival probabilities displayed in Figure 6 for two consecutive subperiods lasting 25 years each. The two subperiods do not show considerable differences.

[20] Figure 6 shows that the empirical survival probability exhibits hyperbolic tails at durations of 1, 4, 10 and 24 h. The lower bounds $x_{\min}$ and slopes α are computed using the method described in section 2. Figure 6 emphasizes that, at any duration between 1 and 24 h, the hyperbolic tail has an approximately constant slope, while the variability of the series with respect to the mean decreases with the accumulation duration. The lower bound $x_{\min}$ above which the power law behavior holds depends on the rainfall duration. If $x_{\min}$ is the limit of the hyperbolic tail and the simple scaling holds at this point, $x_{\min}$ should scale as a function of the accumulation duration such that the absolute quantile is a constant.

[21] Therefore, the highest rainfall rates of this long series display simple scaling properties for durations in between 1 and 24 h. If the rainfall rate is a random process $X(t)$ ($t \in \Re$), we are able to magnify or contract by a factor λ the highest rates without modifying the distribution shape [*Sornette*, 2004, p. 148]. As stated by *Gupta and Waymire* [1990], we can compute a scale function $\lambda^{\theta} \geq 0$ such that

$$X(\lambda t) \stackrel{d}{=} \lambda^{\theta} X(t). \tag{7}$$

[22] The equality in distribution (equation (7)) is referred to as "strict sense simple scaling." It is obvious in Figure 6 that the strict sense simple scaling does not apply to the whole rainfall rate distribution (also stated by *Gupta and Waymire* [1990]) which is rather multifractal [*Hubert et al.*, 1993; *Tessier et al.*, 1993]. However, this is not incompatible with the simple scaling behavior observed for the highest rainfall rates. Several studies showed evidences of the simple scaling behavior of very high quantiles, such as annual maxima of the rainfall rate [*Burlando and Rosso*, 1996; *Bendjoudi et al.*, 1997; *Menabde et al.*, 1999; *Borga et al.*, 2005] while other authors reported a change in the high rainfall quantile behavior that *Schertzer and Lovejoy* [1992] define as "multifractal phase transition."

4. Regionalization of the Power Law Exponent

4.1. Study Region and Data

[23] The Cévennes-Vivarais region is located in the southeast of France (see Figure 1). This region is prone to heavy rainfall events causing flash floods [*Jacq*, 1994; *Delrieu et al.*, 2005]. Typical meteorological conditions have been detected as triggering conditions for flash floods, mainly the advection of warm humid air from the south.

[24] The region is southerly bounded by the Mediterranean sea providing warm and humid air masses. The Alps massif to the east and the Massif Central to the west channel the flow in the Rhône River valley (eastern boundary of the study region). The Massif Central mountain range, approximately oriented north-northwest, is impacted by low- level air masses from south and favors their lifting. The northwestern part of the study region, usually less concerned by severe rainfall events, is constituted by flat highlands.

[25] The rain gage network in the region has been installed at the beginning of the previous century. However, digitized hourly rainfall data are available only since 1993. In this study, we used data from 1993 to 2008 provided by the French Meteorological Service Météo-France. From 1993 to 2000 about 150 rain gages were available; this number increased to about 200 after the year 2000 (date of implementation of the Hydrometeorological Survey Service, OHMCV [*Delrieu*, 2004]). The rain gage density is very fluctuating from one place to another (see Figure 1) and the mean rain gage density is approximately 1 per 150 km^2.

4.2. Methodology and Implementation

[26] The hyperbolic behavior and self-similarity of the distributions of heavy rainfall intensities cumulated over periods from 1 to 24 h have been empirically assessed in section 3. In the current section, we regionalize the parameters characterizing the self-similarity of heavy rainfall rates at different durations.

[27] The steps involved in the estimation of the power law exponent α at a rain gage are the following.

[28] 1. Select a rain gage having at least 2000 nonzero observations at the duration $D = 1h$.

[29] 2. Cumulate the rain gage observations over higher accumulation durations through a fixed-window process; we cumulated at 2, 4 and 8 h.

[30] 3. Fr D = 1h, estimate $x_{\min}$ by minimizing the D statistics of the Kolmogorov-Smirnov test (for each value of x_1, a value of α is computed and the statistics D is returned).

[31] 4. Estimate the quantile of $x_{\min}$ in the complete rainfall series (both zero and positive values)

[32] 5. For each duration $D > 1h$, $X_{\min}$ is computed as the value of x_D corresponding to the same quantile as for $D = 1$ h.

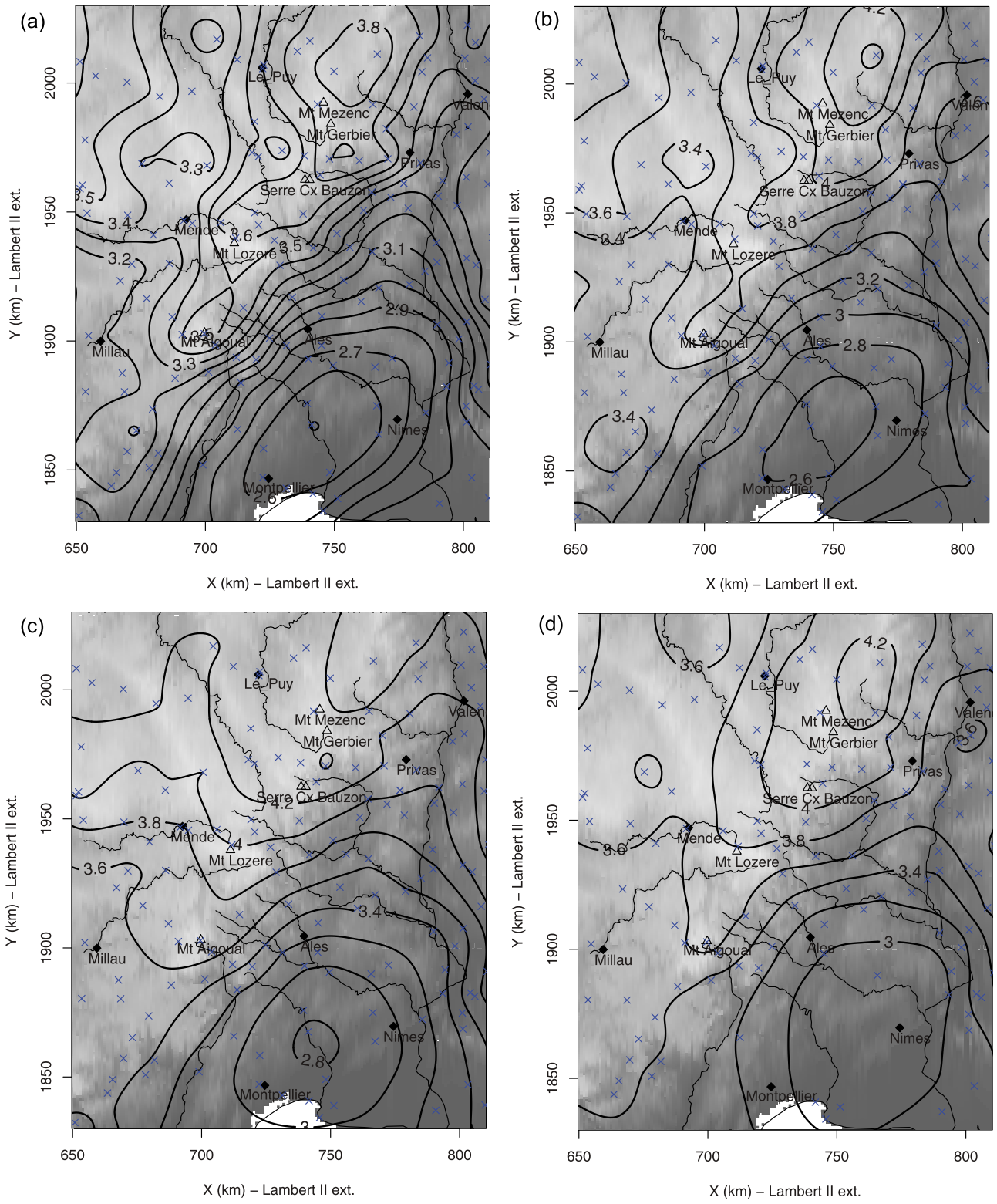

Figure 7. Power law exponent ($\hat{\alpha}$) map in the region of interest for different accumulation periods: (a) D = 1 h, (b) D = 2 h. (c) D = 4 h, and (d) D = 8 h. The crosses represent the considered rain gage network at the corresponding duration. See Figure 1 for details on the background.

[33] 6. Compute α with the method proposed by *Clauset et al.* [2009] taking $X_{\min}$ as the lower bound, following equation (2).

[34] The interpolated exponent $\hat{\alpha}_1$ of the point rainfall for the 1 h duration is mapped in Figure 7a, clearly showing elongated structures corresponding to the mountain ridge. The regionalization of $\hat{\alpha}$ is obtained by interpolation, performed only if the variable has a definite correlation structure. The universal kriging method (described by *Chiles and Delfiner* [1999]) has been chosen to interpolate the values of

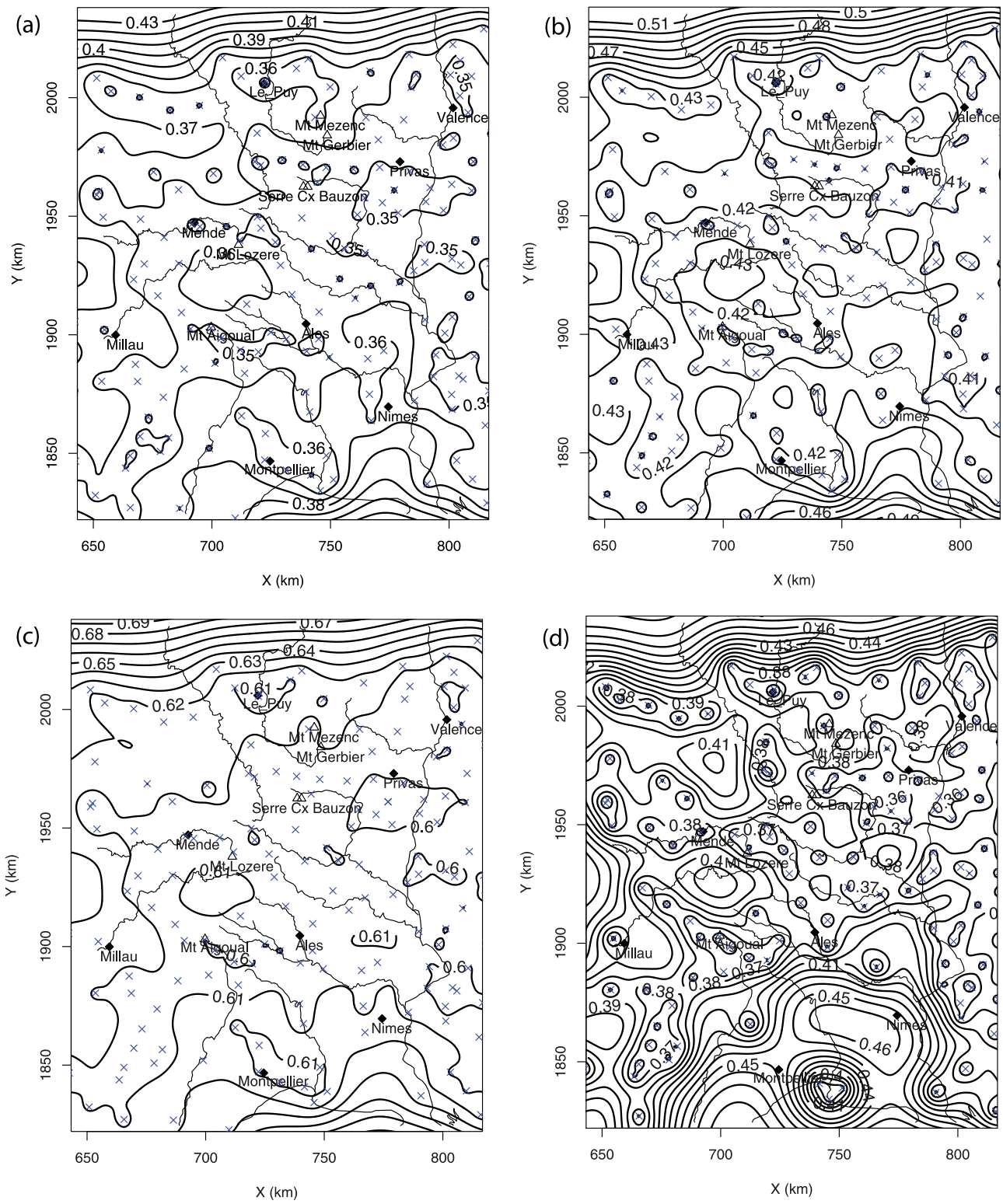

Figure 8. Kriging standard deviation map for the α exponent: (a) D = 1 h, (b) D = 2 h. (c) D = 4 h, and (d) D = 8 h.

$\hat{\alpha}$ at different accumulation times. We emphasize that even though the value of $\hat{\alpha}_1$ has been spatially interpolated, it remains a local measure. Since different mechanisms are involved, the integration of α over a surface does not correspond to the areal power law exponent.

[35] The interpolated $\hat{\alpha}_1$ values can be altered by two kinds of errors. One is due to the interpolation process; the second is due to the assumption of hyperbolic behavior of rainfall distribution tails and their fitting. The former is evaluated through the kriging standard deviation displayed in Figure 8a. Figure 8a shows that except in the domain

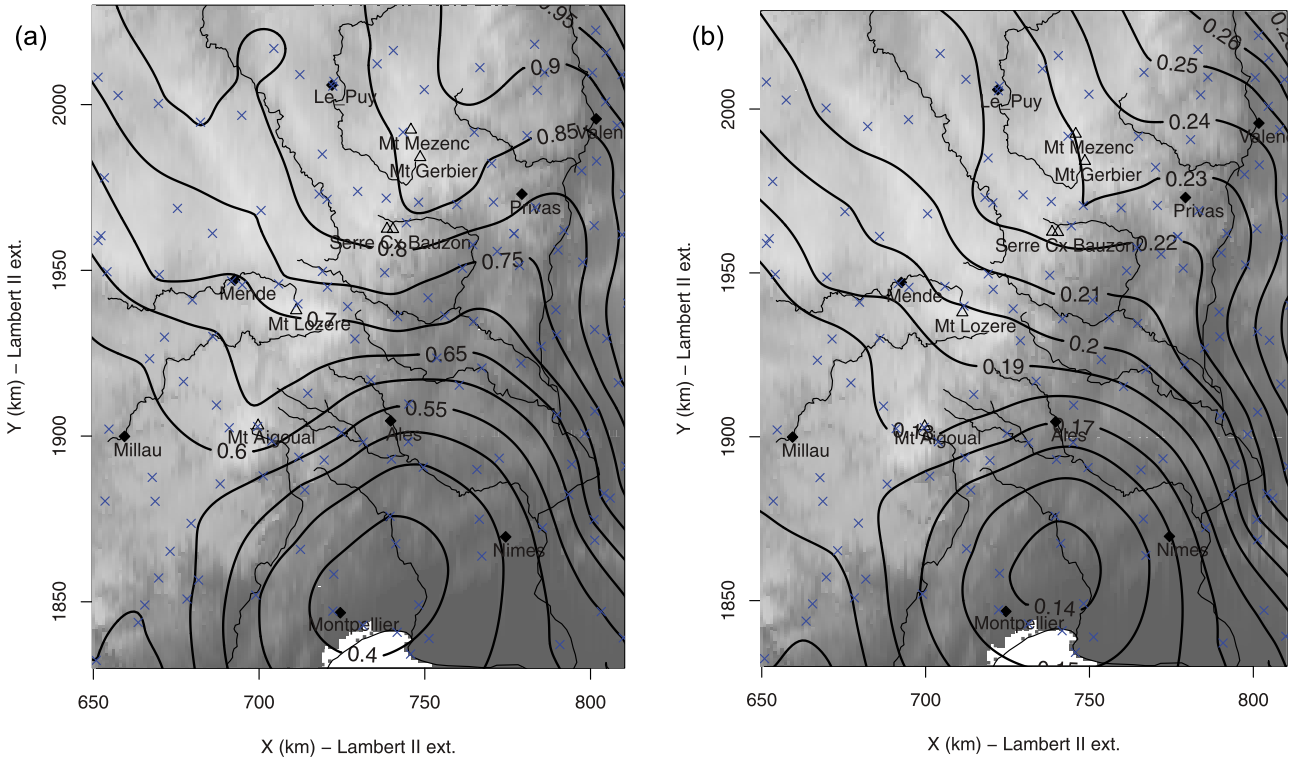

Figure 9. Confidence interval of $\hat{\alpha}_1$ for the 95% confidence level: (a) absolute confidence interval and (b) confidence interval relative to $\hat{\alpha}_1$. The maps have been obtained by kriging interpolation.

fringe, the kriging standard deviation is lower than 10% of $\hat{\alpha}_1$ which we consider as acceptable in comparison, for instance, to the variation of 20% of $\hat{\alpha}$ across the region. The confidence interval $\Delta\hat{\alpha}$ efficiently assesses the latter error type (i.e., the reliability of the point $\hat{\alpha}$ estimation). In Figure 9a, the confidence interval $\Delta\hat{\alpha}$ for the 95% confidence level is mapped for the region of interest. Figure 9b shows that the confidence interval roughly varies between 14% in the plain region to 26 % of $\hat{\alpha}$ in the northern part of the region of study. The α estimation is the most reliable in the southern part of the study region. The lowest $\hat{\alpha}_1 \sim 2.6$ are located at the lowest altitude and increase gradually with altitude up to the Cévennes-Vivarais mountain ridge ($\hat{\alpha}_1 \sim 3.6$) and the Alps. In the Rhône river valley the gradient is weaker. We have to point out that, in the mountainous subregion, the power law model is less adapted to the series, as shown by analyzing the confidence interval (Figure 9b). In section 4.3, we will evaluate the α exponent for the accumulation periods of 2, 4 and 8 h.

4.3. Regional Rainfall Scaling Assessment

[36] Following methodology described in the previous paragraph, the assessment of the simple scaling assumption is undertaken in the whole study region by evaluating the α behavior at different accumulation periods. At each rain gage, rainfall rates are aggregated over 2, 4 and 8 h periods using nonoverlapping windows. The 4 h limit guarantees sufficiently long rainfall series (>500) while, for the 8 h interval, most of gages had been discarded due to the poor sample set size.

[37] Since the quantile of $x_{\min}$ is assumed to be scale invariant (section 2), this property has been used to retrieve its values at the 2, 4 and 8 h durations from $x_{\min}$ computed at the 1 h duration. Using the maximum likelihood estimation method (2), $\hat{\alpha}_2$, $\hat{\alpha}_4$ and $\hat{\alpha}_8$ are estimated (section 2) and mapped (section 4.2, Figures 7b, 7c, and 7d).The interpolation variance associated to the $\hat{\alpha}_2$, $\hat{\alpha}_4$ and $\hat{\alpha}_8$ kriging is almost identical in pattern and displays increasing values of the estimation error with duration (Figures 8b, 8c, and 8d). This is due to the decreasing sample set size and to the reduced number of available gages. Despite those sources of uncertainties, $\hat{\alpha}_2$, $\hat{\alpha}_4$ and $\hat{\alpha}_8$ remain approximately constant in the subregion corresponding to the lowest altitudes. On the contrary, the fluctuations seem more consistent near the mountain ridge and in the northwest plateau. This evidence validates the scaling behavior of heavy rainfall for short duration in this flat subregion in agreement with *Hubert and Bendjoudi* [1996]. In the subregion at the north of the Mont Lozère, α varies consistently with duration. The simple scaling hypothesis does not hold in this area.

[38] Figure 10 shows the map of $x_{\min}$ for D = 1 h. In the plain region and over the Massif Central, the lower bound $x_{\min}$ is the lowest (~4 mm h^{-1}) and increases toward the northwest over the mountain slope until the ridge up to about 9 mm h^{-1} and toward the north up to 8 mm h^{-1}. Mountainous and northeastern rain gages show the smallest proportion of events lying in the hyperbolic part of the distribution. This is the main evidence of the effect of orography on rainfall from the point of view of the probability distribution.

5. Concluding Remarks

[39] The paper has shown that an objective method can be used to characterize the heavy rainfall distribution featuring

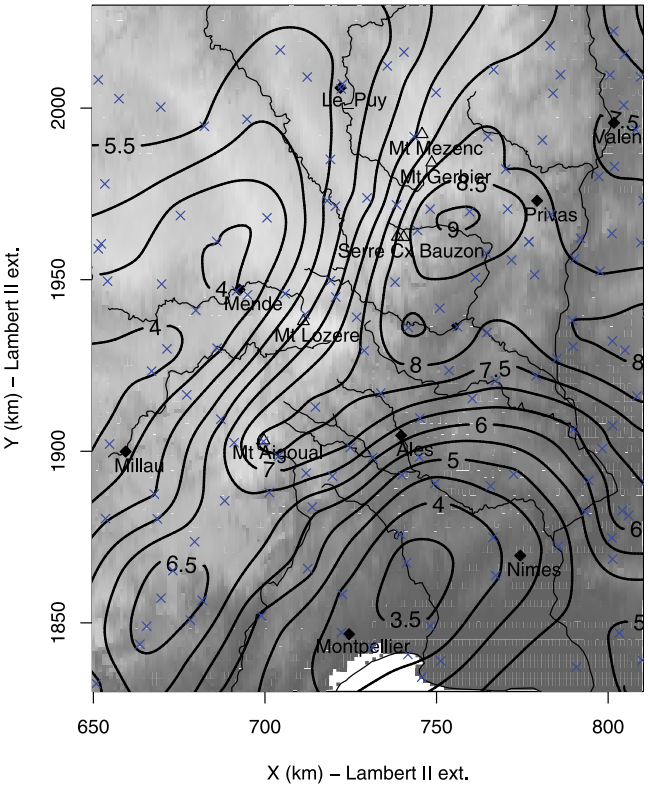

Figure 10. Map of the power law lower bound $\hat{x}_{\min}$ for $D = 1$ h.

hyperbolic tails. The objective and unbiased determination of the power law exponent α is necessary for the regionalization of the power law behavior of rainfall series. This process has been repeated at different accumulation periods, leading to the definition of a subregion where the power law exponent is approximately constant. Considering the relatively short observation period (16 years), we assume that no significant trends affecting the stationarity of the rain gage series are present.

[40] In section 5.1, we will interpret the results from the point of view of the physical processes generating rainfall within the study region, and we will discuss the current findings regarding the statistical analysis of extreme rainfall events.

5.1. Physical Interpretation of the Results

[41] The behavior of rainfall distribution tails is heterogeneous in the region of interest. The regionalization of the rainfall variability (α values, Figure 7), the agreement between the power law model and the tail distribution shape (confidence interval, Figure 9) and the proportion of observations concerned by the power law behavior ($x_{\min}$ values, Figure 10) delineate the differences between the flat area and the mountainous region. In the southeast subregion (between Alès, Nîmes and Montpellier) the rainfall variability, i.e., the ratio between maximum and average rainfall, is the highest at short durations: it is the area where the power law model is the most adapted (lower confidence interval in Figure 9) and the number of observations exhibiting hyperbolic tails is the highest (lower $x_{\min}$ in Figure 10). The power law exponent in the region shows a relief-oriented gradient: both the Central Massif and the Alps exhibit high α, corresponding to lower rainfall variability compared to the flat areas. The signature of the Rhône Valley is sharp for small accumulation periods, decreasing for high accumulation periods.

[42] Several studies [*Sénési et al.*, 1996; *Ducrocq et al.*, 2002; *Ricard*, 2002; *Ducrocq et al.*, 2003; *Delrieu et al.*, 2005; *Nuissier et al.*, 2008] have shown that the heaviest rainfall are yielded by mesoscale systems entering the region from the south and southeast. Grossly speaking, the relatively warm and humid air masses coming from the Mediterranean sea are lifted upward by an orographic barrier, the Massif Central slopes, and by thermodynamical mechanisms (cold pool [*Nuissier et al.*, 2008]) which block the heaviest rainfall in the southeast of the study region.

[43] The south-north gradient, displayed by the statistical properties of heavy rainfall in the northern part of the study area especially for accumulation periods higher than 2 h, is less linked to the relief. Both valley and mountain slopes are present in the region. The lack of references concerning the rainfall events occurring in this region allows only hypothetical reasoning. The average increase of α values in this region corresponds to a general decrease of rainfall variability compared to the southern portion. An interpretation may be that, besides the relief effect, the distance from the storm-triggering zone plays an important role on the weakening of the storm convection, due to the ground friction. In conclusion, the sheltering effect generated by the relief is not the only factor limiting the rainfall variability.

5.2. Consequences for the Extreme Modeling

[44] The representativity of the power law exponent α for the description of the variability of heavy rainfall is demonstrated by two main results. First, α has a well-determined spatial structure (Figure 7). The interpolation process has been easily performed since the variable has a definite empirical variogram at any duration. Interesting properties of α are that whatever the accumulation duration, α is always lower in the flat area; in addition, in the southern portion of the domain, α is approximately constant with the accumulation duration, satisfying the necessary conditions for the simple scaling of heavy rainfall. As recalled in section 1, the cumulative probability distributions of extreme rainfall intensities are usually modeled either by generalized extreme value (GEV) or generalized Pareto distributions (GPD) [*Kottegoda and Rosso*, 1997; *Sornette*, 2004] depending on the selection of heavy rainfall events (maxima or peaks over threshold). Depending on their parameters, both the GEV and GPD distributions may display exponential or power law tails. Extreme rainfall analyses related to design rainfall assessment in the southeast of France [*Guillot and Duband*, 1967; *Slimani and Lebel*, 1986; *Nguyen Thao et al.*, 1993; *Cernesson et al.*, 1996] and elsewhere [*Zhang and Singh*, 2007], for instance, assumed that infradaily extreme rainfall intensities follow Gumbel distributions (GEV-I), i.e., exponential survival probability tails. Thick tail distributions have been found in space-time rainfall fluctuations [*Kumar and Foufoula-Georgiou*, 1993; *Perica and Foufoula-Georgiou*, 1996].

[45] *Koutsoyiannis* [2003] pointed out some reasons of the GEV-I popularity in hydrology: design-rainfall studies are based on maxima analyses, GEV-I exhibit linearity on Gumbel diagrams. on the log-log plot in Figure 2. More-

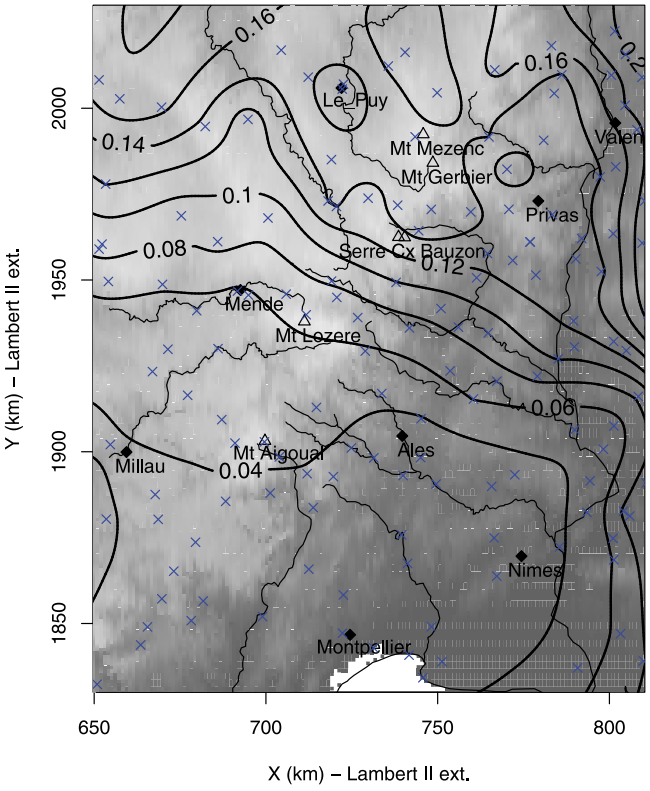

Figure 11. Stability of the power law exponent: variance of the $\hat{\alpha}$ values at 1, 2, 3, and 4 h.

over, GEV-II (Fréchet) distribution has one additional parameter respect to GEV-I, giving larger uncertainties with limited sample sets. However, several studies reported that GEV-I underestimates actual extreme rainfall intensities (see *Koutsoyiannis* [2003] for a detailed description). In this study most of rain gages shows hyperbolic tails at various durations: this is an evidence of the Fréchet behavior of maxima; the exponential behavior of survival probability tails typical of Gumbel distribution is not in agreement with our findings concerning the southern part of the study region. Considering the proportion of hyperbolically distributed samples at the accumulation time of 1 h, we observed that in most of rain gages they are no more than 5 % of the positive rainfall values. This value corresponds to the 0.1–0.3% of the whole observations, meaning that in a year, between 8 and 20 observations are hyperbolically distributed. However, the strong interdependence of most of these values further limits the number of independent data lying in the hyperbolic tail. In addition, increasing the accumulation period, the number of observations per year decreases, reducing the number of hyperbolically distributed samples. In the case of the 24 h accumulation period, we should observe in average a hyperbolic sample every three years. In our opinion, this explains why a limited sample set of daily data better fits a GEV-I distribution rather than a GEV-II one.

[46] The most important result in this paper is the assessment of the variability of α with duration (Figure 11). The variance among the α values at 1 h, 2 h, 3 h, 4 h is used as indicator of the variability of the temporal scaling properties of heavy rainfall. The 8 h accumulation period has not been considered in this computation: many stations have been discarded due to the poor sample set size. The lower the variance, the higher the reliability in the temporal simple scaling behavior. Figure 11 shows that, in a large subregion covering both the flat area and a portion of the foothill (southern part of the study region), the variability of α with the accumulation period is small (variance lower than 0.06). In this zone α can be considered as a constant with respect to duration. Since in the same subregion the confidence interval of the power law estimation is lower than 20% of the value of α (Figure 9), in these areas the rainfall distribution can be considered approximately self-similar in the power law distributed part. In the framework of the usual extreme value analysis, this means that the "extreme value index" ξ, (which is 0 in GEV-I and equal to $\frac{1}{\alpha}$ in GEV-II), would always be higher than 0 in this subregion and, even more noteworthy, it is constant with duration. In regions where time simple scaling of heavy rainfall holds, the derivation of one of the three parameters of GEV-II by means of scale invariance relations can therefore determine a considerable improvement in the fitting of limited samples series with GEV-II distribution.

[47] **Acknowledgments.** This work has been supported by the Vulnerability, Environment and Climate (VMC) program of the French National Agency for Research (ANR). The project is entitled "Forecast and Projection in Climate Scenario of Mediterranean Intense Events: Uncertainties and Propagation on Environment" (MedUP). Data have been collected by the French weather service Météo-France. The authors are grateful to the reviewers for their constructive remarks.

References

Bendjoudi, H., P. Hubert, and D. Schertzer (1997), Interpretation multifractale des courbes intensité-durée-fréquence des précipitations, *C. R. Acad. Sci., Ser. IIa Sci. Terre Planetes*, *2*, 323–326.

Borga, M., C. Vezzani, and G. Dalla Fontana (2005), Regional rainfall depth-duration-frequency equations for an alpine region, *Nat. Hazards*, *36*, 221–235.

Burlando, P., and R. Rosso (1996), Scaling and multiscaling models of depht-duration-frequency curves for storm precipitation, *J. Hydrol.*, *187*, 45–64.

Cernesson, F., J. Lavabre, and J. Masson (1996), Stochastic model for generating hourly hyetographs, *Atmos. Res.*, *42*, 149–161.

Chiles, J., and P. Delfiner (1999), *Geostatistics Modeling Spatial Uncertainty*, John Wiley, New York.

Clauset, A., C. Shalizi, and M. Newman (2009), Power-law distributions in empirical data, *SIAM Rev.*, (51), 661–703.

Delrieu, G. (2004), L'Observatoire Hydro-météorologique Méditerranéen Cévennes-Vivarais (the Cévennes-Vivarais Mediterranean Hydro-meteorological Observatory), *Houille Blanche*, *6*, 83–88.

Delrieu, G., et al. (2005), The catastrophic flash-flood event of 8–9 September 2002 in the Gard region, France: A first case study for the Cévennes-Vivarais Mediterranean Hydro-meteorological Observatory, *J. Hydrol.*, *6*, 34–52.

Ducrocq, V., D. Ricard, J. Lafore, and F. Orain (2002), Storm-scale numerical rainfall prediction for five precipitating events over France: On the importance of the initial humidity field, *Weather Forecast.*, *17*, 1236–1256.

Ducrocq, V., G. Aullo, and P. Santurette (2003), Précipitations intenses et les inondations des 12 et 13 Novembre 1999 sur le sud de la France, *Meteeorologie*, *42*, 18–27.

Frisch, U., and G. Parisi (1985), Fully developed turbulence and intermittency, in *Turbulence and Predictability in Geophysical Fluid Dynamics and Climate Dynamics*, edited by M. Ghil et al., pp. 84–88, North-Holland, Amsterdam.

Goldstein, M., S. Morris, and G. Yen (2004), Problems with fitting to the power-law distributions, *Eur. Phys. J. B*, *41*, 255–258.

Guillot, P., and D. Duband (1967), La méthode du GRADEX pour le calcul de la probabilité des crues à partir des pluies, in *Colloque International sur les Crues et Leur Évaluation*, *IAHS Publ.*, *7*, 560–569.

Gumbel, E. (1958), *Statistics of Extremes*, Columbia Univ. Press, New York.

Gupta, V., and E. Waymire (1990), Multiscaling properties of spatial rainfall and river flow distributions, *J. Geophys. Res.*, *95*(D3), 1999–2009.

Hubert, P., and H. Bendjoudi (1996), Introduction à l'étude des longues séries pluviométriques, paper pressented at XIIèmes Journées Hydrologiques, Off. de la Rech. Sci. et Tech. d'Outre-Mer, Montpellier, France, 10–11 Oct.

Hubert, P., Y. Tessier, S. Lovejoy, P. Ladoy, J. Carbonner, S. Violette, and I. Desurosne (1993), Multifractals and extreme rainfall events, *Geophys. Res. Lett.*, *20*(10), 931–934.

Jacq, V. (1994), Inventaire des situations à précipitations diliviennes sur les régions Languedoc-Roussillon, PACA et Corse, période 1958–1994, *Tech. Rep. 3*, Météo-France, Paris.

Kottegoda, N., and R. Rosso (1997), *Probability and Reliability for Civil and Environmental Engineers*, Blackwell, Oxford, U. K.

Kotz, S., and S. Nadarajah (2000), *Extreme Value Distributions: Theory and Applications*, Imp. Coll. Press, London.

Koutsoyiannis, D. (2003), On the appropriateness of the Gumbel distribution for modelling extreme rainfall, paper presented at LESC Exploratory Workshop, Eur. Sci. Found., Bologna, Italy.

Koutsoyiannis, D., D. Kozonis, and A. Manetas (1998), A mathematical framework for studying rainfall intensity-duration-frequency relationships, *J. Hydrol.*, *206*, 118–135.

Kumar, P., and E. Foufoula-Georgiou (1993), A new look at rainfall fluctuations and scaling properties of spatial rainfall using orthogonal wavelets, *J. Appl. Meteorol.*, *32*, 209–222.

Ladoy, P., F. Schmitt, D. Schertzer, and S. Lovejoy (1993), Variabilité temporelle multifractale des observations pluviométriques à Nîmes, *C. R. Acad. Sci., Ser. III*, *317*, 775–782.

Menabde, M., A. Seed, and G. Pegram (1999), A simple scaling model for extreme rainfall, *Water Resour. Res.*, *35*(1), 335–339.

Nguyen Thao, T. P. N. G., P. Bois, and J. A. Villasenor (1993), Simulation in order to choose a fitting method for extreme rainfall, *Atmos. Res.*, *30*, 13–36.

Nuissier, O., V. Ducrocq, D. Ricard, C. Lebeaupin, and S. Anquetin (2008), A numerical study of three catastrophic precipitating events over western mediterranean region (Southern France): Part I: Numerical framework and synoptic ingredients, *Q. J. R. Meteorol. Soc.*, *134*(630), 111–130.

Perica, S., and Foufoula-Georgiou (1996), Model for multiscale disaggregation of spatial rainfall based on coupling meteorological and scaling descriptions, *J. Geophys. Res.*, *101*(D21), 26,347–26,361.

Ricard, D. (2002), Initialisation et assimilation de données à méso-échelle pour la prévision à haute résolution des pluies intenses de la région Cévennes-Vivarais (in French), Ph.D. thesis, Univ. Pierre Sabatier-Toulouse III, Toulouse, France.

Schertzer, D., and S. Lovejoy (1987), Physically based rain and cloud modeling by anisotropic, multiplicative turbulent cascades, *J. Geophys. Res.*, *92*(D8), 9692–9714.

Schertzer, D., and S. Lovejoy (1992), Hard and soft multifractal processes, *Physica A*, *185*, 187–194.

Sénési, S., P. Bougeault, J. Chèze, P. Cosentino, and R. Thepenier (1996), The Vaison-la-Romaine flash flood: Mesoscale analysis and predictability issues, *Weather Forecast.*, *11*, 417–442.

Sivakumar, B. (2000), Fractal analysis of rainfall observed in two different climatic regions, *Hydrol. Sci. J.* , *45*(5), 727–738.

Slimani, M., and T. Lebel (1986), Comparison of three methods of estimating rainfall frequency parameters according to the duration of accumulation, in *International Symposium on Flood Frequency and Risk Analyses*, edited by J. V. Singh, pp. 277–291, D. Reidel, Dordrecht, Netherlands.

Sornette, D. (2004), *Critical Phenomena in Natural Sciences*, Springer, Berlin.

Tessier, Y., S. Lovejoy, and D. Schertzer (1993), Universal multifractals: Theory and observations for rain and clouds, *J. Appl. Meteorol.*, *32*(2), 223–250.

Zhang, L., and V. P. Singh (2007), Gumbel-Hougaard copula for trivariate rainfall frequency analysis, *J. Hydrol. Eng.*, *12*(4), 409–419, doi:10.1061/(ASCE)1084-0699(2007)12:4(409).

D. Ceresetti, J.-D. Creutin, and G. Molinié, Laboratoire d'Étude des Transfert en Hydrologie et Environnement, Université de Grenoble, BP 53, F-38041 Grenoble CEDEX 9, France. (gilles.molinie@ujf-grenoble.fr)